

12-1-2010

Mechanism of N-methylation by the tRNA m1G37 methyltransferase Trm5.

Thomas Christian
Thomas Jefferson University

Georges Lahoud
Thomas Jefferson University

Cuiping Liu
Thomas Jefferson University


Katherine Hoffmann
University of California at Santa Barbara

John J Perona
University of California at Santa Barbara

See next page for additional authors

[Let us know how access to this document benefits you](#)

Follow this and additional works at: <http://jdc.jefferson.edu/bmpfp>

 Part of the [Biochemistry Commons](#), [Medical Biochemistry Commons](#), and the [Molecular Biology Commons](#)

Recommended Citation

Christian, Thomas; Lahoud, Georges; Liu, Cuiping; Hoffmann, Katherine; Perona, John J; and Hou, Ya-Ming, "Mechanism of N-methylation by the tRNA m1G37 methyltransferase Trm5." (2010). *Department of Biochemistry and Molecular Biology Faculty Papers*. Paper 26.
<http://jdc.jefferson.edu/bmpfp/26>

This Article is brought to you for free and open access by the Jefferson Digital Commons. The Jefferson Digital Commons is a service of Thomas Jefferson University's [Center for Teaching and Learning \(CTL\)](#). The Commons is a showcase for Jefferson books and journals, peer-reviewed scholarly publications, unique historical collections from the University archives, and teaching tools. The Jefferson Digital Commons allows researchers and interested readers anywhere in the world to learn about and keep up to date with Jefferson scholarship. This article has been accepted for inclusion in Department of Biochemistry and Molecular Biology Faculty Papers by an authorized administrator of the Jefferson Digital Commons. For more information, please contact: JeffersonDigitalCommons@jefferson.edu.

Authors

Thomas Christian, Georges Lahoud, Cuiping Liu, Katherine Hoffmann, John J Perona, and Ya-Ming Hou

As submitted to:

RNA

And later published as:

**“Mechanism of N-methylation
by the tRNA m¹G37 methyltransferase Trm5”**

Volume 16, Number 12, pp. 2484-92.

October 27, 2010

doi: 10.1261/rna.2376210

**Thomas Christian[†], Georges Lahoud[†], Cuiping Liu[†],
Katherine Hoffmann[‡], John J. Perona^{‡*}, and Ya-Ming Hou^{†*}**

[†]Department of Biochemistry & Molecular Biology, Thomas Jefferson University,

233 South 10th St., Philadelphia PA 19107

[‡]Department of Chemistry & Biochemistry, University of California at Santa

Barbara, Santa Barbara CA 93106-9510

*Corresponding authors: J. J. Perona (perona@chem.ucsb.edu) and

Y. M. Hou (ya-ming.hou@jefferson.edu)

Short title: Mechanism of tRNA methylation by Trm5

Keywords: anticodon loop, S-adenosylmethionine (AdoMet), pH-rate profile, active site assembly

ABSTRACT

Trm5 is a eukaryal and archaeal tRNA methyltransferase that catalyzes methyl transfer from S-adenosylmethionine (AdoMet) to the N¹ position of G37 directly 3' to the anticodon. While the biological role of m¹G37 in enhancing translational fidelity is well established, the catalytic mechanism of Trm5 has remained obscure. To address the mechanism of Trm5 and more broadly the mechanism of N-methylation to nucleobases, we examined the pH-activity profile of an archaeal Trm5 enzyme, and performed structure-guided mutational analysis. The data reveal a marked dependence of enzyme-catalyzed methyl transfer on hydrogen ion equilibria: the single-turnover rate constant for methylation increases by one order of magnitude from pH 6.0 to reach a plateau at pH 7.0. This suggests a mechanism involving proton transfer from G37 as the key element in catalysis. Consideration of the kinetic data in light of the Trm5-tRNA-AdoMet ternary cocrystal structure, determined in a precatalytic conformation, suggests that proton transfer is associated with an induced fit rearrangement of the complex that precedes formation of the reactive configuration in the active site. Key roles for the conserved R145 side-chain in stabilizing a proposed oxyanion at G37-O⁶, and for E185 as general base to accept the proton from G37-N¹, are suggested based on the mutational analysis.

INTRODUCTION

The methylation of proteins and nucleic acids at nitrogen plays key roles in regulating gene expression. In proteins, recent work has established the importance of lysine and arginine methylation for controlling biological activities (Bedford and Clarke 2009; Ng et al. 2009). Methylation at one or multiple positions of these side chains alters charge distribution, hydrogen bonding, and steric properties, and thus is well suited to regulate the assembly and interactions of macromolecular complexes. In nucleic acids, methylation occurs at nearly all non-glycosidic nitrogens in the canonical nucleobases, including the guanosine N³, which is methylated in wybutosine after an additional ring is added to the original base (Noma et al. 2006). The only positions that have no methylation found so far are the adenosine N³ and N⁷. Nucleobases with N-methylation are particularly prevalent in structural RNAs, most commonly tRNA and rRNA, accounting for a subset of the over 100 known modified nucleosides (Czerwoniec et al. 2009). However, despite the large variety of chemical and structural contexts in which these RNA N-methylation events occur, and their well-established importance in regulation of protein synthesis (Gustilo et al. 2008), little is known regarding the mechanisms of the enzyme-catalyzed reactions. Only the N-methyltransferases M.EcoRI and M.TaqI, which catalyze formation of m⁶A in DNA as part of bacterial restriction-modification systems, have been studied in any detail to date (Mashhoon and Reich 1994; Goedecke et al. 2001; Newby et al. 2002).

The m¹G37 modification in the tRNA anticodon loop is conserved in all three domains of life (Supplementary Fig. S1), and plays an important role in increasing fidelity of ribosomal decoding in both the cytoplasm and mitochondria (Bjork et al. 1989; Bjork et al. 2001; Lee et al. 2007). In methanogens, m¹G37 is also essential for tRNA recognition by phosphoseryl- and cysteinyl-tRNA synthetases (Liu et al. 2007; Smith et al. 2008). In all organisms, the synthesis of m¹G37 is catalyzed by the AdoMet-dependent tRNA(m¹G37) methyltransferase, with *S*-adenosyl homocysteine (AdoHcy) as the second product. Interestingly, the bacterial enzyme TrmD and

archaeal/eukaryal enzyme Trm5 feature distinct tertiary folds in their active-site domains, suggesting that they have evolved separately (Ahn et al. 2003; Elkins et al. 2003; Goto-Ito et al. 2008; Goto-Ito et al. 2009). TrmD and Trm5 also recognize different determinants on tRNA: **Trm5 requires full integrity of the L-shaped tRNA structure for activity, whereas TrmD requires only the D-stem and anticodon stem-loop motifs in the vertical arm (Christian and Hou 2007).**

Trm5 from *Methanocaldococcus jannaschii* is the lead model system for elucidating the enzyme-catalyzed mechanism of m¹G37 formation (Christian et al. 2004; Christian et al. 2006; Christian and Hou 2007). Crystal structures of the enzyme reveal that it is a member of the class I amino-methyltransferase family (Goto-Ito et al. 2008; Goto-Ito et al. 2009), which transfers the methyl group from AdoMet to nitrogen in widely different chemical environments. Trm5 features a conserved NLPK motif in the active site, a variant of the consensus NPPY motif in other class I amino-methyl transferases. Kinetic studies show that the rate-limiting step in the catalytic cycle of Trm5 occurs after formation of m¹G37 on the enzyme (Christian et al. 2006; Christian et al. 2010), similar to other class I methyltransferases ((Flynn et al. 1996; Bhattacharya and Dubey 1999; Vilkaitis et al. 2001). The crystal structure of *M. jannaschii* Trm5 bound to tRNA and AdoMet reveals a conformation poised for catalysis (Goto-Ito et al. 2009), in which the N¹ of G37 is located 2.8 Å from the methyl group of AdoMet. However, although the high pK_a (~9.5) of the guanine N¹ suggests that enzyme-catalyzed deprotonation would be necessary for methyl transfer, there is no apparent general base positioned to accept this proton. Thus, the mechanism for methyl transfer remains unclear despite the detailed structural information.

To directly address the role of proton transfer in the Trm5 mechanism, we have determined the pH-dependence of the methylation event as it occurs in the enzyme active site. To our knowledge, this is the first such study for an endocyclic N-methylation reaction on nucleic acids. The data reveal that catalysis by Trm5 is indeed dependent on hydrogen ion equilibria, and suggest that proton transfer from N¹ of G37 is necessary to activate the enzyme. Together with

the crystal structures of Trm5 and structure-guided mutational analysis, these data place fundamental constraints on the enzyme mechanism and emphasize the importance of an induced-fit process after the initial tRNA binding event to form the reactive configuration required for methyl transfer. Importantly, two strictly conserved residues in the Trm5 family, R145 and E185, have been identified by sequence analysis. The roles of these amino acids in rate enhancement are addressed by structure-guided mutational analysis.

RESULTS AND DISCUSSION

pH-dependent methyl transfer by *M. jannaschii* Trm5

To measure the pH-dependence of *M. jannaschii* Trm5 reactivity, we determined the single-turnover rate constant for methyl transfer under conditions of saturating AdoMet and tRNA, with molar excess of enzyme over tRNA. The advantage of single turnover (as compared to steady state) assays is that the observed rate constant (k_{obs}) must correspond to either the chemical step (k_{chem}) or a closely linked induced-fit conformational rearrangement prior to catalysis (k_{conf}) in the following reaction scheme:



Here ES* represents a Trm5-tRNA-AdoMet ternary complex that has undergone an induced-fit conformational change, so that the reactive substrate moieties are poised for catalysis.

Measurements of the pH-dependence of the single-turnover rate constant were exhaustively controlled, and the quality of the tRNA substrate was rigorously monitored. An *in vitro* transcript of *M. jannaschii* tRNA^{Cys} was refolded by annealing (Supplementary Fig. S1), and its integrity as a Trm5 substrate verified by demonstrating a capacity for methylation to ~70% levels in extended time courses (e.g. pH 6.0, 8.1, and 9.8, Supplementary Figs. S2a, b). Saturating conditions were established at 7.5 μM Trm5, 0.5 μM tRNA^{Cys}, and 25 μM [³H]-AdoMet at pH 6.0, 8.1 and 9.8. All reactions were carried out at 55°C with Trm5 present in 15-fold molar excess

over tRNA. Further controls established that the order of mixing and the nature of the buffer do not influence the rates. Finally, we also demonstrated that pre-incubation of Trm5 at pH 6.0, followed by adjustment of the solution to pH 8.0, does not cause irreversible inactivation of the enzyme. Enzyme treated in this manner retained equivalent activity in single-turnover assays.

Time courses of [³H]-methyl group transferred to tRNA were best fit to a single exponential function at all values of pH, yielding k_{obs} . The plot of k_{obs} against pH shows a steep increase in the rate of methyl transfer as the proton concentration is lowered, up to an asymptote at pH 7.0 (Fig. 1a). The logarithmic plot of k_{obs} ($\log(k_{\text{obs}})$) against pH reveals a slope of 0.92 (Fig. 1b), indicating a mechanism involving the deprotonation of one ionizing group. The data are most consistent with the anticipated deprotonation of N¹ of G37 and are well fit to the equation:

$$k_{\text{obs}} = \frac{k_{\text{A}^-} + k_{\text{AH}} 10^{pK_a - \text{pH}}}{1 + 10^{pK_a - \text{pH}}}$$

where k_{obs} is the observed reaction rate at a specific pH, k_{AH} is the activity of the protonated form of G37 ($k_{\text{AH}} = 0$), k_{A^-} is the activity of the deionized form of G37, and K_a is the equilibrium constant for the dissociation of the proton (Fersht 1999). An optimal fit of the data ($R^2 = 0.98$) yields $pK_a = 6.5 \pm 0.1$, roughly three units below the pK_a of the N¹ proton of guanosine in solution (Clauwaert and Stockx 1968). Shifts of pK_a values of this magnitude and larger have been well documented for other enzymes (Frey and Hegeman 2007). However, it should be noted that a definitive assignment of the pK_a to the deprotonation of G37-N¹ is not possible based on this experiment alone.

Proposed mechanism of methyl transfer by Trm5

Although the identity of the transferred proton cannot be unambiguously established at present, the dependence of the reaction rate on proton removal is consistent with a mechanism in which the observed rate constant (k_{obs}) corresponds to nucleophilic attack on the methyl group of AdoMet by the deprotonated N¹ of G37 in tRNA, with electron transfer to the sulfonium

ion (Fig. 2). Proton abstraction from G37 N¹ could be facilitated by an enzyme residue functioning as a general base, with a shift of electron density from the N-H bond to the O⁶ of the guanine ring. The electron sink at O⁶ is important for promoting the initial proton removal from N¹, while a positively charged enzyme side chain could stabilize the increased electron density at O⁶. Interestingly, interplay between endocyclic position 1 and exocyclic position 6 in purines was previously noted for N⁶ methylation of adenine, where methylation at N¹ occurs first, followed by methyl migration to N⁶ via the base-catalyzed Dimroth rearrangement, involving ring opening of the adenine base (Engel 1975).

The crystal structure of the Trm5-tRNA-AdoMet ternary complex reveals that the methyl group has not been transferred from AdoMet to G37 (Goto-Ito et al. 2009), perhaps because reactivity is greatly reduced at the low temperature of crystallization compared with the optimal 85 °C growth temperature of *M. jannaschii*. For the following reasons, it also appears likely that the crystal lattice has trapped a deprotonated form of G37 with the N¹ nitrogen in an sp²-hybridized state, in which the lone pair of electrons is poised to attack the AdoMet methyl group (Fig. 2). First, G37 N¹ is located only 2.8 – 3.0 Å from the electrophilic methyl group of AdoMet, so that an interstitial proton may be sterically excluded. Second, the adjacent positively charged sulfonium group of AdoMet likely also disfavors approach by protonated N¹. Finally, despite the demonstrated importance of proton equilibria to catalysis (Fig. 1), the structure does not reveal an appropriately positioned general base that might abstract the N¹ proton (see Fig. 3a). This consideration suggests that proton abstraction from N¹ occurs prior to the configuration observed in the crystal lattice, which represents a state that is clearly poised for catalysis. Thus, proton removal would have occurred during the induced-fit conformational rearrangement leading to juxtaposition of G37 with AdoMet. The implication is that the pH dependence of k_{obs} in single-turnover analysis corresponds to proton transfer during a slower process of induced fit, rather than the bond-breaking and bond-forming steps of methyl transfer (that is, the measured rate constant k_{obs} corresponds to k_{conf} in the above scheme, and not to k_{chem}).

Structure-guided mutational analysis of Trm5

As a test of this proposed mechanism, we used structure-guided mutational analysis of *M. jannaschii* Trm5 to elucidate the identities of amino acids that may directly facilitate methyl transfer. Mutant enzymes were constructed and analyzed by single turnover assays with saturating AdoMet and increasing molar ratio of enzyme to tRNA to determine the K_d for tRNA and the saturating rate constant k_{obs} (summarized in Table 1). **Importantly, all of the mutational effects were associated with alteration of k_{obs} , rather than K_d , indicating that the driving force for activity and specificity is associated with the first order induced-fit and chemical steps of the reaction scheme, rather than the binding of tRNA.** Mutational effects were interpreted by examining the relevant functional groups in the enzyme binary complex with the AdoMet analog sinefungin (Goto-Ito et al. 2008) and in the ternary complex with AdoMet and tRNA, where the base of G37 becomes unstacked from its neighbors in the anticodon loop and flips into the active site (Fig. 3a) (Goto-Ito et al. 2009). Comparison of binary and ternary complex structures was used to gain insight into how insertion of the guanine base into the active site affects the positioning of functional groups.

Structure-based sequence alignments show that the only two strictly conserved residues among Trm5 enzymes are R145 and E185 (Supplementary Fig. S3A and S3B). Comparison of the binary and ternary Trm5 complexes shows that R145 is located on a mobile surface loop that markedly changes conformation upon tRNA binding. In the tRNA-bound enzyme, R145 orients its guanidinium group toward the Hoogsteen face of the flipped-out G37 base, allowing donation of two H-bonds to the O⁶ and N⁷ groups (Fig. 3b). The interaction between conserved R145 and O⁶ of G37 supports the proposed mechanism (Fig. 2), suggesting that the function of this positively charged residue is to stabilize the negative charge on O⁶ in the initial step. The

R145A mutation reduces k_{obs} by 20-fold, demonstrating the importance of this arginine in facilitating rate enhancement.

Unlike R145, the position and conformation of E185 within the core catalytic domain are not greatly altered upon binding of tRNA G37 in the active site (Fig. 3b). This strictly conserved glutamate does not directly bind either substrate, but is located immediately N-terminal to R186, which does reorient in the ternary complex to stabilize AdoMet binding by forming a charged hydrogen bond with the carboxylate group of the methyl donor. The position of E185 adjacent to the active site, together with its strict conservation in all known Trm5 enzymes and the solution pK_a of 4.3 for the side-chain carboxylate, suggest that E185 may function as the general base for removal of the G37-N¹ proton, and that proton abstraction catalyzed by this residue occurs together with the induced-fit conformational change leading to the fully assembled active site that is visualized in the crystal structure. The properties of the E185A and E185Q mutants support this hypothesis, because the single-turnover k_{obs} measured for these enzymes is decreased by 300 and 60-fold, respectively, compared with the wild-type (WT) Trm5. (Table 1). The more than 3-fold improved activity of E185Q compared with E185A suggests that E185 is crucial both for general base catalysis and for the conformational change that precedes catalysis. In contrast, E185D, which retains the capacity to function as a general base ($pK_a = 3.7$), is reduced only 2.4-fold in k_{obs} compared with WT Trm5. Similar to WT Trm5, analysis of the pH-activity dependence of the E185D mutant also reveals a plot of $\log(k_{\text{obs}})$ against pH with a slope of 1.0 and a pK_a of 6.6 ± 0.2 (Supplementary Fig. S4). WT and E185D Trm5 each therefore appear to function by the same mechanism. Further, the high k_{obs} retained by E185D supports the notion that this parameter corresponds to an induced-fit conformational change, because the flexibility required for motion of the protein and RNA groups relative to each other should allow retraction of the carboxylate by the length of a carbon-carbon bond, while still permitting the juxtaposition required for proton transfer.

Induced-fit for active-site assembly

To further test whether R145 or E185 function in active-site assembly, we evaluated their roles in AdoMet binding using pre-steady-state burst kinetics, as described previously (Christian et al. 2010). In this assay, the kinetics of m¹G37 synthesis is monitored under conditions of saturating tRNA and molar excess of AdoMet over enzyme, to permit one round of methyl transfer on the enzyme, followed by steady state turnovers. WT Trm5 exhibits a burst of rapid product synthesis in the first turnover, followed by a slower and linear phase reflecting the rate-limiting product release step. Analysis of the amplitude of the burst phase as a function of AdoMet concentration then allows estimation of the binding affinity of Trm5 to AdoMet (Table 2). While WT Trm5 exhibits K_d (AdoMet) of $0.4 \pm 0.1 \mu\text{M}$, identical to the value reported previously (Christian et al., 2010), the R145A and E185D mutations elevate K_d (AdoMet) by 10-fold and 11-fold, respectively (Table 2). Since neither R145 nor E185 directly bind AdoMet, these data suggest that each of these catalytically crucial residues are also involved in active-site assembly. Coupling of AdoMet binding to catalysis is also revealed by the properties of the R186A mutant, for which k_{obs} is decreased by 12-fold (Table 1; Fig. 3b). Notably, *instead of R186 in archaeal Trm5, sequence homology analysis reveals that eukaryotic organisms have conserved H186 (Supplementary Fig.S3A and S3B). While H186 in principle could act as a general base for proton abstraction of G37, it is unlikely to perform this function in the presence of a functional E185, due to the strict conservation of the latter residue and the much stronger effect on k_{obs} brought about by its mutation (>300-fold by E185A, Table 1). The role of H186 in eukaryotic Trm5 enzymes is presently unknown.*

To provide a more complete assessment of catalytic function, we also examined the roles of other highly conserved residues in the active site (Table 1, Fig. 3). The NLPK loop is of central interest, because of its conserved role in stabilizing AdoMet among class I amino-methyl transferases. In the ternary Trm5-tRNA^{Cys}-AdoMet complex, the side-chain amide of N265 accepts a hydrogen bond from the exocyclic 2-NH₂ of G37, while P267 stacks on the guanine ring (Fig. 3c). Although both residues move slightly away from AdoMet upon G37 binding,

mutations of N265 had only modest effects on k_{obs} (0.8-, 6-, and 12-fold reduction for N265H, N265Q, and N265A, respectively), whereas mutations of P267 had much more severe effects (120-fold reduction for P267A, P267A/N265Q, and P267A/N265H). The near-WT activity of N265H, which may retain a hydrogen-bond acceptor at an equivalent spatial position, reveals the importance of the hydrogen bond with G37-N². However, the stronger effect of the mutations containing P267A suggests a key role for this proline in coordinating the active site rearrangement. Y177 stabilizes G37 by stacking on the opposing side relative to P267 (Figs. 3c, 3d). The Y177A mutation produces a 60-fold decrease in k_{obs} , while the Y177F mutant retains near-WT activity. These findings demonstrate that the hydrogen bond formed by the Y177 hydroxyl group with the 2'-OH of the G37 ribose is not crucial to rate enhancement. We also found that the N265A and Y177A mutations increase K_{d} for AdoMet by 2.5-fold and 12-fold, respectively (Table 2). The effect of the Y177A mutation on AdoMet binding again reveals structural coupling between the tRNA-G37 and AdoMet binding sites.

The side-chain carboxylate of D223 contacts both the 2'- and 3'-OH groups of the adenosine ribose of AdoMet, and this residue also remains relatively unchanged in its spatial position upon tRNA binding (Fig. 3c). **Removal of the carboxylic side chain of D223 resulted in either a severe loss in k_{obs} (D223A, 170-fold) or complete loss of activity (D223N and D223L, >1,200 fold),** whereas activity was preserved in D223E (Table 1). These data are consistent with conservation of D223 in the Trm5 family, since the only other naturally occurring alternative is the substitution of aspartate with glutamate. The D223A mutation, which destabilizes the ribose moiety of AdoMet, also increased the K_{d} for AdoMet by 22-fold to $8.8 \pm 1.3 \mu\text{M}$. While the properties of the D223 mutants, considered alone, suggest the possibility that this residue might function as the catalytic base, we favor E185 in this role, for two reasons. First, as described above, E185 is appropriately positioned to accept a proton from G37-N¹ during the induced-fit transition, while D223 binds a distal portion of AdoMet and is not located near the reactive moieties. Second, D223 is conserved as an AdoMet-binding residue in many class I

methyltransferases that function to catalyze methyl transfer at a variety of chemically diverse positions on the nucleobases. A role in acid-base catalysis for Trm5 thus appears less plausible.

Several of the mutations studied here have been previously examined by steady state analysis (Christian et al. 2006). In all case, the mutational effects on k_{cat} were significantly smaller than the corresponding effects on k_{obs} . For example, the R145A mutation reduced k_{cat} by 2.5-fold (*vs* k_{obs} by 20-fold); the Y177A mutation reduced k_{cat} by 6.2-fold (*vs* k_{obs} by 60-fold); the D223A mutation reduced k_{cat} by 25-fold (*vs* k_{obs} by 170-fold); the N265A mutation reduced k_{cat} by 6.2-fold (*vs* k_{obs} by 12-fold); and the P267A mutation reduced k_{cat} by 83-fold (*vs* k_{obs} by 120-fold). In each case, the k_{cat} value is also smaller in magnitude than the respectively measured k_{obs} value, suggesting that for these mutants the k_{cat} corresponds to a step after methyl transfer, as demonstrated for the WT enzyme (Christian et al. 2010). The smaller k_{cat} effect as compared to the k_{obs} effect thus suggests a lesser role of the specific residue in product release. All of the mutations for which steady-state kinetics were measured also display a larger effect on K_{m} for tRNA (6-12-fold), than on the tRNA binding affinity (< 2-fold). This is consistent with product release being the rate-limiting step, since K_{m} represents a complex combination of rate and equilibrium constants in this case. Interpretation of the pre-steady-state data is more straightforward, because the fundamental rate and equilibrium constants are directly measured, giving unambiguous insight into the effects of mutations.

We also used single turnover assays to assess the roles of several positively charged residues that interact with or lie adjacent to the tRNA anticodon loop backbone near the active site. For example, K318 forms a salt bridge to the phosphate of A38, R181 forms a salt bridge to the phosphate at U39 and to the D-arm backbone at positions C25/G26), and the side-chain of K137 is reoriented toward solvent upon tRNA binding (Fig. 3d). Alanine substitutions of these three residues were created and mutant enzymes were evaluated for their performance in tRNA binding and methyl transfer kinetics. Among these mutants, the largest effect was observed for R181A, for which k_{obs} is reduced by 20-fold, suggesting that the bridging interaction between the

anticodon loop and the coaxially stacked D-arm is important for catalysis, probably by facilitating the induced-fit rearrangement. K137A is reduced in k_{obs} by 4-fold, suggesting a smaller role in the induced-fit process. Surprisingly, the K318A mutation had no effect on k_{obs} despite its interaction with an adjacent phosphate that might have been expected to participate in the flipping of the G37 base into the active site.

Conclusion

This work addresses how Trm5 catalyzes deprotonation of the N¹ of G37 to enable methyl transfer from AdoMet. In principle, deprotonation of N¹ might be envisioned to occur simply from its approach toward the positively charged sulfonium group of AdoMet, without invoking the need for a general base. In this case, the role of the enzyme would be entirely to stabilize the bound substrates and to juxtapose the deprotonated nitrogen and the electrophilic methyl group. However, based on the strong mutational effect of the strictly conserved E185 and R145 residues on k_{obs} for methyl transfer, the data presented here support the reaction mechanism for methyl transfer outlined in Fig. 2, in which E185 acts as the general base that abstracts the proton from N¹ of G37, while R145 lowers the transition-state free energy by interacting with the incipient negative charge on O⁶. This proposed mechanism now provides the basis for further experiments to clarify specific details. For example, the use of guanine base analogs will be useful in more definitively establishing whether the measured $\text{p}K_{\text{a}}$ of 6.5 ± 0.1 associated with pH-dependent methyl transfer (Fig. 1) indeed corresponds to the downward shift in $\text{p}K_{\text{a}}$ for the N¹ of G37, as we have hypothesized.

An important finding is that, while neither E185 nor R145 form a direct interaction with the methyl donor in the ternary complex, both residues enable AdoMet binding, suggesting that both play a further key role in promoting active-site assembly. Active-site organization is also facilitated by coordinated conformational changes of the residues that organize binding to the G37 base (i.e. Y177, N265, and P267) and those that stabilize AdoMet (i.e. R186, N265, and

D223). Additional residues (i.e. K318 and R181) appear to be involved in shaping the tRNA backbone in the D-anticodon arm, so as to facilitate stable insertion of G37 into the active site. The involvement of diverse enzyme side chains in the active site suggests that the induced fit rearrangement of the enzyme-tRNA-AdoMet complex is elaborate, coupling both short- and long-range interactions to arrive at the reactive configuration of the complex. The assignment of the proton transfer to the induced-fit rearrangement makes it particularly challenging to identify the residues or motifs that are the key determinant in the process. Further work to develop a fluorescence approach to directly monitor the induced-fit process will be necessary and beneficial to gain insight into this process.

The large catalytic defect of the E185A mutant, demonstrated by a reduction of k_{obs} by greater than 300-fold, reflects loss of both the catalytic carboxylate group and most of the aliphatic portion of the side chain. Because the E185Q mutant remains severely defective with a loss of 60-fold in k_{obs} compared to the WT enzyme, it appears that acid-base catalysis plays a major role in rate enhancement. This notion is distinct from methylation at DNA adenine-N⁶ by M.TaqI, which is instead critically dependent on substrate organization for rate enhancement (Newby et al. 2002). An additional distinction is that, while deprotonation of G37-N¹ by Trm5 occurs early, and the nucleophilic attack on AdoMet is by nitrogen in the sp^2 hybridization state (Fig. 2), deprotonation by M.TaqI occurs only after the nitrogen has acquired significant sp^3 character (Goedecke et al. 2001; Newby et al. 2002), due to the much higher pK_a (~20) of adenine N⁶. Consistent with this analysis, a pH kinetic analysis of the m⁶A DNA methylase M.EcoRI showed only a linear 4-fold change in k_{obs} over a wide pH range (Mashhoon and Reich 1994). Based on these two examples, it appears that enzymatic methylation at exocyclic adenine N⁶ may depend less on acid-base chemistry for rate acceleration than methylation at endocyclic guanine N¹. Further studies of additional methyltransferases will be necessary to test this prediction.

This work provides a benchmark that will be useful as a model for parallel investigations of the proton transfer mechanisms of other amino methyl transferases that operate on structural RNAs. An important example is the m¹G37 synthesis reaction catalyzed by the bacteria-specific TrmD enzyme, which shares no structural homology with Trm5 and so must develop a distinct stereochemical pathway for the same chemical reaction. Other examples include amino methyl transfer reactions that target chemically distinct positions to synthesize m¹A, m⁶A, m²G, m²₂G, m⁷G, and m⁴C, all of which are widely present in nucleic acids and contribute to the central process of gene expression.

MATERIALS AND METHODS

Expression and purification of *M. jannaschii* Trm5 and tRNA^{Cys}.

M. jannaschii Trm5 with a C-terminal His-tag sequence was expressed in the vector pET-22b in *E. coli* BL21(DE3)/RIL cells. Protein expression was induced by addition of 0.3 mM IPTG to the growing cultures at A_{600} between 0.4 and 0.6. Trm5-containing cells were lysed by sonication, and the enzyme purified by heating of the cell extract to 75°C for 20 min to precipitate native proteins, followed by metal-affinity (Talon, ClonTech) and Q Sepharose chromatography steps (Christian et al. 2006). Active-site titration of the purified enzyme based on the amplitude in the burst assay revealed ~50% active fraction (Christian et al. 2010), which was used to correct the enzyme concentration as determined from the Bradford assay. To prepare tRNA for kinetic analysis, the *M. jannaschii* tRNA^{Cys} gene was transcribed from a duplex DNA template constructed from complementary synthetic oligonucleotides containing a 10-bp overlapping region, which were then extended using the Klenow fragment of *E. coli* DNA polymerase (Sherlin et al. 2001). Transcription reactions were carried out as previously described for synthesis of *M. mazei* tRNA^{Cys} transcripts, except that 2'-O methyl sugar modifications at the two 5' nucleotides of the non-coding strand were omitted (Liu et al. 2007). RNA was recovered by ethanol precipitation, resuspended in 10 mM Tris-HCl (pH 7.5), and heated to 85°C for 3 min. MgCl₂ was then added to 2 mM final concentration, and the reactions were slow-cooled to room temperature to maximize refolding.

Single-turnover methylation assays

Methylation at the N¹ position of G37 in *M. jannaschii* tRNA^{Cys} transcripts was assayed at 55°C, the highest temperature compatible with retention of structure in the RNA (optimal growth temperature of *M. jannaschii* at 85°C). Determination of kinetic parameters K_d (tRNA) and k_{obs} by single turnover kinetic assays, and determination of the kinetic K_d (AdoMet) by pre-steady-state assays were as described (Christian et al. 2010), using ³H-labeled S-AdoMet (67.3

Ci/mmol, Perkin Elmer). Reactions were initiated by addition of tRNA. Aliquots taken at specific time points were precipitated with 5% (w/v) trichloroacetic acid on filter pads, washed extensively, and air-dried prior to scintillation counting. Data were background-subtracted and corrected for a quenching efficiency of approximately 60%. Curve fitting to the equation for a single ionizing system (see Results and Discussion) was performed with Kaleidagraph.

Measurement of pH-dependent methyl transfer activity

Buffers used in the pH-dependent measurements were as follows: sodium cacodylate (pH 6.0); MES (pH 6.0, 6.1, 6.2, 6.4, 6.5, 6.6); MOPS (pH 6.6, 6.7, 6.9, 7.1); glycyl glycine (pH 7.1, 7.3, 7.5, 8.1, 8.6, 8.7); glycine (pH 8.7, 9.3, 9.8). Each buffer was made as a 5x solution (0.5 M buffer, 0.5 M KCl, 30 mM MgCl₂, 0.5 mM EDTA), mixed with a 5x solution B (20 mM DTT and 0.12 mg/mL BSA), and diluted to 1x to check the pH. If the pH was lower than the normal value, drops of 5 M KOH were added to the 5x solution such that the 1x solution became properly adjusted. This adjustment was particularly important for pH values of 6.6 and lower, because measurements of activity without the adjustment failed to reveal the full activity at low pH values. Uncorrected measurements at low pH values led to the previous suggestion that a slope of 2 characterizes the log k_{obs} versus pH plot (Hou and Perona 2010). No differences in rate were observed for reactions run at pH values where two different buffers were used. Reactions at pH lower than 6.6 were monitored by hand sampling, while those at higher pH values were monitored using a rapid quench apparatus (Kintek RQF-3). For single turnover condition, *M. jannaschii* Trm5 enzyme was used at 7.5 μM (15-fold molar excess of tRNA) as the active concentration and was added to one syringe at 55 °C containing final concentration of 0.1 M buffer, 0.1 M KCl, 6 mM MgCl₂, 0.1 mM EDTA, 4 mM DTT, and 0.024 mg/mL BSA. Upon rapid mixing with 0.5 μM tRNA^{Cys} (previously heat-cooled and annealed) and 25 μM AdoMet in the same buffer from the second syringe at 55 °C, the time course of the reaction was monitored. Substrate saturation at pH 6.0, 8.1, and 9.8 was shown by measuring k_{obs} in reactions for which

the enzyme and tRNA concentrations were each reduced by a factor of two, while maintaining enzyme concentrations in 15-fold molar excess. Control reactions for order of addition were carried out at pH 6, 8 and 10; no significant differences in measured rates were observed. The consistency in the measured k_{obs} across all three pH values establishes that both the tRNA and AdoMet substrates are stable at all relevant pH values. The resistance of the tRNA substrate to alkaline degradation was further confirmed by analysis on a 12% PAGE/7M urea gel. Standard deviations are plotted in Figure 1.

ACKNOWLEDGMENTS

We thank Tom Bruice, Eugene Mueller, and Philip Bevilacqua for helpful discussion, and Eric Wickstrom for assistance in utilizing the 3-D projection environment for molecular design and surgical simulation supported by USAMRMC W81XWH-09-1-0577. This work was supported by NIH grants GM53763 (to J.J.P.) and GM81601 (to Y.M.H.).

References

- Ahn HJ, Kim HW, Yoon HJ, Lee BI, Suh SW, Yang JK. 2003. Crystal structure of tRNA(m¹G37)methyltransferase: insights into tRNA recognition. *Embo J* **22**(11): 2593-2603.
- Bedford MT, Clarke SG. 2009. Protein arginine methylation in mammals: who, what, and why. *Mol Cell* **33**(1): 1-13.
- Bhattacharya SK, Dubey AK. 1999. Kinetic mechanism of cytosine DNA methyltransferase MspI. *J Biol Chem* **274**(21): 14743-14749.
- Bjork GR, Jacobsson K, Nilsson K, Johansson MJ, Bystrom AS, Persson OP. 2001. A primordial tRNA modification required for the evolution of life? *Embo J* **20**(1-2): 231-239.
- Bjork GR, Wikstrom PM, Bystrom AS. 1989. Prevention of translational frameshifting by the modified nucleoside 1-methylguanosine. *Science* **244**(4907): 986-989.
- Christian T, Evilia C, Hou YM. 2006. Catalysis by the second class of tRNA(m¹G37) methyltransferase requires a conserved proline. *Biochemistry* **45**(24): 7463-7473.
- Christian T, Evilia C, Williams S, Hou YM. 2004. Distinct origins of tRNA(m¹G37) methyltransferase. *J Mol Biol* **339**(4): 707-719.
- Christian T, Hou YM. 2007. Distinct determinants of tRNA recognition by the TrmD and Trm5 methyl transferases. *J Mol Biol* **373**(3): 623-632.
- Christian T, Lahoud G, Liu C, Hou YM. 2010. Control of catalytic cycle by a pair of analogous tRNA modification enzymes. *J Mol Biol* **400**(2): 204-217.
- Clauwaert J, Stockx J. 1968. Interactions of polynucleotides and their components. I. Dissociation constants of the bases and their derivatives. *Z Naturforsch B* **23**(1): 25-30.
- Czerwoniec A, Dunin-Horkawicz S, Purta E, Kaminska KH, Kasprzak JM, Bujnicki JM, Grosjean H, Rother K. 2009. MODOMICS: a database of RNA modification pathways. 2008 update. *Nucleic Acids Res* **37**(Database issue): D118-121.
- Elkins PA, Watts JM, Zalacain M, van Thiel A, Vitazka PR, Redlak M, Andraos-Selim C, Rastinejad F, Holmes WM. 2003. Insights into catalysis by a knotted TrmD tRNA methyltransferase. *J Mol Biol* **333**(5): 931-949.
- Engel JD. 1975. Mechanism of the Dimroth rearrangement in adenosine. *Biochem Biophys Res Commun* **64**(2): 581-586.
- Fersht AR. 1999. *Structure and mechanism in protein science*. W. H. Freeman and Company, New York.
- Flynn J, Glickman JF, Reich NO. 1996. Murine DNA cytosine-C5 methyltransferase: pre-steady- and steady-state kinetic analysis with regulatory DNA sequences. *Biochemistry* **35**(23): 7308-7315.
- Frey PA, Hegeman A. 2007. *Enzymatic reaction mechanisms*. Oxford University Press, New York.
- Goedecke K, Pignot M, Goody RS, Scheidig AJ, Weinhold E. 2001. Structure of the N⁶-adenine DNA methyltransferase M.TaqI in complex with DNA and a cofactor analog. *Nat Struct Biol* **8**(2): 121-125.
- Goto-Ito S, Ito T, Ishii R, Muto Y, Bessho Y, Yokoyama S. 2008. Crystal structure of archaeal tRNA(m¹G37)methyltransferase aTrm5. *Proteins* **72**(4): 1274-1289.
- Goto-Ito S, Ito T, Kuratani M, Bessho Y, Yokoyama S. 2009. Tertiary structure checkpoint at anticodon loop modification in tRNA functional maturation. *Nat Struct Mol Biol* **16**(10): 1109-1115.

- Gustilo EM, Vendeix FA, Agris PF. 2008. tRNA's modifications bring order to gene expression. *Curr Opin Microbiol* **11**(2): 134-140.
- Hou YM, Perona JJ. 2010. Stereochemical mechanisms of tRNA methyltransferases. *FEBS Lett* **584**(2): 278-286.
- Lee C, Kramer G, Graham DE, Appling DR. 2007. Yeast mitochondrial initiator tRNA is methylated at guanosine 37 by the Trm5-encoded tRNA (guanine-N1)-methyltransferase. *J Biol Chem* **282**(38): 27744-27753.
- Liu C, Gamper H, Shtivelband S, Hauenstein S, Perona JJ, Hou YM. 2007. Kinetic Quality Control of Anticodon Recognition by a Eukaryotic Aminoacyl-tRNA Synthetase. *J Mol Biol.*
- Mashhoon N, Reich NO. 1994. Investigation of ionizable residues critical for sequence-specific enzymatic DNA modification: protein modification and steady-state and pre-steady-state kinetic pH analyses of EcoRI DNA methyltransferase. *Biochemistry* **33**(23): 7113-7119.
- Newby ZE, Lau EY, Bruice TC. 2002. A theoretical examination of the factors controlling the catalytic efficiency of the DNA-(adenine-N6)-methyltransferase from *Thermus aquaticus*. *Proc Natl Acad Sci U S A* **99**(12): 7922-7927.
- Ng SS, Yue WW, Oppermann U, Klose RJ. 2009. Dynamic protein methylation in chromatin biology. *Cell Mol Life Sci* **66**(3): 407-422.
- Noma A, Kirino Y, Ikeuchi Y, Suzuki T. 2006. Biosynthesis of wybutosine, a hyper-modified nucleoside in eukaryotic phenylalanine tRNA. *Embo J* **25**(10): 2142-2154.
- Sherlin LD, Bullock TL, Nissan TA, Perona JJ, Lariviere FJ, Uhlenbeck OC, Scaringe SA. 2001. Chemical and enzymatic synthesis of tRNAs for high-throughput crystallization. *RNA* **7**(11): 1671-1678.
- Smith DR, Quinlan AR, Peckham HE, Makowsky K, Tao W, Woolf B, Shen L, Donahue WF, Tusneem N, Stromberg MP et al. 2008. Rapid whole-genome mutational profiling using next-generation sequencing technologies. *Genome Res* **18**(10): 1638-1642.
- Vilkaitis G, Merkiene E, Serva S, Weinhold E, Klimasauskas S. 2001. The mechanism of DNA cytosine-5 methylation. Kinetic and mutational dissection of HhaI methyltransferase. *J Biol Chem* **276**(24): 20924-20934.

Table 1. Kinetic parameters with respect to tRNA for *M. jannaschii* Trm5.

	K_d (tRNA, μM)	k_{obs} (s^{-1})	k_{obs}/K_d ($\mu\text{M}^{-1}\text{s}^{-1}$)	Rel to WT k_{obs}
WT	0.7 ± 0.1	0.12 ± 0.04	0.17	1.0
R145A	1.0 ± 0.5	0.006 ± 0.001	0.006	1/20
E185A		<0.0004	<0.0004	< 1/300
E185D	0.9 ± 0.3	0.05 ± 0.01	0.056	1/2.4
E185Q	0.8 ± 0.2	0.002 ± 0.0001	0.0025	1/60
R186A	1.2 ± 0.5	0.01 ± 0.001	0.008	1/12
N265A	0.8 ± 0.3	0.01 ± 0.002	0.13	1/12
N265Q	0.8 ± 0.1	0.02 ± 0.004	0.025	1/6
N265H	1.2 ± 0.4	0.15 ± 0.05	0.125	1/0.8
P267A	0.8 ± 0.03	0.001 ± 0.0002	0.0013	1/120
P267A + N265Q	1.4 ± 0.03	0.001 ± 0.0003	0.0007	1/120
P267A + N265H	1.7 ± 0.04	0.001 ± 0.0003	0.0006	1/120
Y177A	1.1 ± 0.6	0.002 ± 0.001	0.002	1/60
Y177F	1.2 ± 0.2	0.09 ± 0.01	0.075	1/1.3
D223A	1.0 ± 0.2	0.0007 ± 0.0002	0.0007	1/171
D223N		< 0.0001		< 1/1,200
D223L		< 0.0001		< 1/1,200
D223E	1.2 ± 0.3	0.14 ± 0.04	0.12	1/0.9
K318A	1.1 ± 0.2	0.11 ± 0.01	0.10	1/1.1
R181A	0.9 ± 0.1	0.006 ± 0.002	0.007	1/20
K137A	1.6 ± 0.4	0.03 ± 0.01	0.019	1/4

Single turnover kinetics was performed by rapid mixing of enzyme (2-25 μM) in one syringe with tRNA (0.25 μM) and AdoMet (25 μM) in the second syringe. Data were fit to the single exponential equation: $y = y_o + A \times (1 - e^{-k_{\text{app}} \times t})$, where y_o is the y intercept, A is the scaling constant, k_{app} is the apparent rate constant, and t is the time in seconds to determine k_{obs} . Control experiments confirmed that the mixing order of enzyme, tRNA, and AdoMet does not affect the rate of methyl transfer. The data of k_{obs} vs. enzyme concentration for single turnover analysis of m1G37-tRNA synthesis were fit to the hyperbolic equation: $y = k_{\text{obs}} \times E_o / (E_o + K_d)$, and E_o is the enzyme concentration. Because mutations generally have little effect on K_d (tRNA), the analysis emphasizes on k_{obs} and the mutational effects relative to the k_{obs} of the WT enzyme (in bold face).

Table 2. Kinetic parameters with respect to AdoMet for *M. jannaschii* Trm5.

	K_d (AdoMet, μM)	k_{obs} (s^{-1})	k_{obs}/K_d ($\mu\text{M}^{-1}\text{s}^{-1}$)	Rel to WT K_d
WT	0.4 ± 0.1	0.12 ± 0.02	0.3	1.0
D223A	8.8 ± 1.3	0.0007 ± 0.0001	8×10^{-5}	1/22
N265A	1.0 ± 0.1	0.01 ± 0.002	0.01	1/2.5
R145A	4.1 ± 0.4	0.006 ± 0.001	0.0016	1/10
E185D	4.4 ± 1.2	0.05 ± 0.01	0.011	1/11
Y177A	4.7 ± 1.4	0.002 ± 0.001	0.00043	1/12

Measurement of the K_d for AdoMet was obtained by pre-steady-state analysis, in which a series of enzyme (5 μM)-AdoMet (0.5-20 μM) complexes (at 37 °C, 30 min) in one syringe was rapidly mixed with tRNA (15 μM , annealed at 37 °C, 15 min) in the second syringe to initiate the m¹G37 synthesis reaction. The burst amplitude as a function of AdoMet concentration was fit to the hyperbolic equation: $y = A \times S / (S + K_d)$; where A is maximum amplitude in burst kinetics, and S is the AdoMet concentration. The analysis emphasizes on K_d (AdoMet) and the mutational effect on this parameter relative to that of the WT enzyme (in bold face).

Figure Legends

Figure 1. pH-dependent methylation by *M. jannaschii* Trm5. (A) Plot of the observed rate constant, k_{obs} , against pH. (B) Logarithmic plot of k_{obs} versus pH.

Figure 2. Proposed mechanism for Trm5. Proton abstraction during docking of G37 in the active site by a general base (E185 in *M. jannaschii* Trm5, upper left) yields deprotonated G37 as visualized in the crystal structure with electron density shifted to O⁶ (stabilized by a positively charged residue, such as R145 in *M. jannaschii* Trm5, upper right). Nucleophilic attack on AdoMet by deprotonated N¹ then leads to product formation.

Figure 3. Structure of the *M. jannaschii* Trm5 active site bound to tRNA and AdoMet. (a) An overall view of the active site, showing all of the residues that have been tested by mutational analysis in this work. (b) Spatial positioning of the catalytic residues R145 and E185 relative to G37 and AdoMet. The position and interactions of the adjacent R186 are also depicted. (c) Detail of the Trm5 active site showing close juxtaposition of G37 N¹ with the AdoMet methyl group. Hydrogen bonds are shown as dotted yellow lines. Key enzyme residues mentioned in the main text are shown in green in the enzyme binary complex with sinefungin, and are shown in red in the enzyme ternary complex with AdoMet and tRNA. Superposition of the two structures was done by aligning sinefungin in the binary complex with AdoMet in the ternary complex, with an rmsd of 0.47 Å of the superimposed atoms. (d) Trm5 residues that stabilize the backbone groups of G37 and A38 in the anticodon loop of the ternary complex. Figures are drawn with PyMol (PDB 2YX1) corresponding to Trm5-sinefungin and with PyMol (PDB 2ZZN) corresponding to the Trm5-tRNA^{Cys}-AdoMet ternary complex (Goto-Ito et al., 2009). H-bonds are shown in yellow dots, while the distance between the N¹ position of G37 and the methyl group of AdoMet is shown in grey.